

+ D. 48816

ANL/ED/CP-98816

RECEIVED  
OCT 19 1999  
OSTI

TEM INVESTIGATION OF A CERAMIC WASTE FORM FOR IMMOBILIZATION OF PROCESS SALTS GENERATED DURING ELECTROMETALLURGICAL TREATMENT OF SPENT NUCLEAR FUEL

Wharton Sinkler, David W. Esh, Thomas P. O'Holleran, Steven M. Frank, Tanya L. Moschetti, Kenneth M. Goff, Stephen G. Johnson  
Argonne National Laboratory - West  
P. O. Box 2528  
Idaho Falls, ID 83404

ABSTRACT

Transmission electron microscopy (TEM) examination is presented of the microstructure of a ceramic waste form developed at Argonne National Lab - West for immobilization of actinides and fission products present in an electrorefiner salt. The material is produced by occluding the salt in zeolite granules, followed by hot isostatic pressing of the occluded zeolite in a mixture with a borosilicate glass. The paper presents results from a cold surrogate ceramic waste form, as well as  $^{239}\text{Pu}$  and  $^{238}\text{Pu}$  loaded samples.

INTRODUCTION

The Spent Fuel Demonstration Project at Argonne National Laboratory concerns disposition of spent driver and blanket fuel from Experimental Breeder Reactor II (EBR II). The EBR II fuel elements are metallic, with 316 stainless steel cladding. Disposition of the fuel needs to satisfy a number of constraints:

- 1) All waste products are environmentally benign
- 2) The loss of usable uranium is minimized
- 3) The process produces a minimum quantity of hazardous by-products

The process which has been developed is based on electrorefinement of the spent fuel at Argonne National Lab - West (ANL-W) [1]. The electrorefinement uses a KCl-LiCl eutectic molten salt bath as an electrolyte. By passing a current through the cell the spent fuel anode is separated into three distinct forms. The first is recovered uranium, deposited on the cathode. Secondly, the cladding and noble metal fission products remain at the anode. Finally, a number of components of the spent fuel accumulate in the electrolyte salt. These are principally Pu, Cs, Na and traces of rare earth fission products. After processing the equivalent of 100 driver fuel assemblies (400 kg), the salt is removal for disposal.

Safe disposal of the electrorefiner salt is in many respects the most challenging aspect of spent fuel disposition using Argonne's electrorefiner process. In order to reduce the amount of water-soluble free chlorides, a process has been developed at Argonne for occlusion of the salt into a zeolite 4A ( $\text{Na}_{96}\text{Al}_{96}\text{Si}_{96}\text{O}_{384}$ ), followed by blending with a glass frit and hot isostatically pressing (HIP) to produce a monolithic ceramic waste form (CWF). A transition of zeolite 4A to sodalite ( $\text{Na}_4\text{Al}_3\text{Si}_3\text{O}_{12}\text{Cl}$ ) occurs in the final HIP.

## **DISCLAIMER**

**This report was prepared as an account of work sponsored by an agency of the United States Government. Neither the United States Government nor any agency thereof, nor any of their employees, make any warranty, express or implied, or assumes any legal liability or responsibility for the accuracy, completeness, or usefulness of any information, apparatus, product, or process disclosed, or represents that its use would not infringe privately owned rights. Reference herein to any specific commercial product, process, or service by trade name, trademark, manufacturer, or otherwise does not necessarily constitute or imply its endorsement, recommendation, or favoring by the United States Government or any agency thereof. The views and opinions of authors expressed herein do not necessarily state or reflect those of the United States Government or any agency thereof.**

## **DISCLAIMER**

**Portions of this document may be illegible in electronic image products. Images are produced from the best available original document.**

Waste form qualification studies commenced with investigations of cold surrogate materials, in which the rare earth element cerium was substituted for plutonium. Subsequently, a  $^{239}\text{Pu}$  loaded ceramic was investigated, and finally a  $^{238}\text{Pu}$  sample was examined, which is part of a longer-term investigation of irradiation effects due to  $\alpha$ -decay in the CWF. In this paper, microstructure and phase content of the cold surrogate, the  $^{239}\text{Pu}$ -loaded and the  $^{238}\text{Pu}$ -loaded samples are described.

## EXPERIMENTAL

The processing and compositional data for the samples investigated are presented in Tables 1-4. In the initial processing step, zeolite 4A is blended with a salt. Three distinct salt compositions were used for the cold surrogates, the  $^{239}\text{Pu}$  sample, and the  $^{238}\text{Pu}$  sample. Salt blending was performed above the salt liquidus temperature. Subsequently the salt-blended zeolite was ground together with a borosilicate glass frit in proportions of 3:1 or 1:1 blended zeolite to glass. Several cold surrogate samples were investigated. Some were produced by HIP at production scale while other cold samples as well as both Pu-loaded samples were produced in a laboratory-scale hot uniaxial press (HUP). Typical conditions for HIP and HUP samples are given in Table 1. No systematic microstructural differences were found between samples produced by HIP and HUP.

TEM sample preparation was performed by sectioning the samples using a diamond saw and core drilling 3 mm disks from the sections. The 3 mm disks were then ground to a thickness of approximately 100  $\mu\text{m}$ , dimpled to a central thickness of  $<20\ \mu\text{m}$  and thinned to perforation in an ion mill using 5 keV  $\text{Ar}^+$ . Prior to observation, samples were coated with a thin ( $\approx 30\ \text{\AA}$ ) layer of amorphous carbon to prevent sample charging. TEM investigations were performed using a JEOL 2010 TEM operated at 200 kV.

## RESULTS AND DISCUSSION

### a) Cold Surrogate CWF

Fig. 1 shows a TEM bright field image (BFI) taken from a surrogate CWF produced by HIP. The image is typical of the cold surrogate samples. As seen in the image, the microstructure of the cold surrogate CWF is dominated by two types of regions, as has also been confirmed using scanning electron microscopy (SEM) [2]. The first consists of polycrystalline sodalite regions with grain sizes ranging from 200 nm to 1  $\mu\text{m}$ , and the second an amorphous glass phase. Sodalite and glass are by far the most significant phases in the samples in terms of volume fraction. Figs. 2 and 3 show typical energy dispersive x-ray spectrometry (EDX) spectra from the glass and sodalite phases, and sodalite was also identified from transmission electron diffraction (TED). From the traces, it is evident that significant interaction of both phases with the surrogate electrolyte salt has occurred. With respect to the initial zeolite Na-Al-Si-O composition, the sodalite phase shows the presence of a significant quantity of Cl, and the glass phase has absorbed both Na and K, as well as a small amount of Cl. Lithium, which cannot be detected by EDX, as well as other trace elements in Table 2, are also probable components of both these phases. The absorption of salt components by the sodalite and glass phases is central to the function of the CWF. The microscopic and spectroscopic confirmation of chloride absorption complements leach tests which indicate a pronounced reduction in the overall quantity of free chlorides in the finished waste form with respect to the starting materials [3].

In addition to the sodalite and glass phases, Fig. 1 shows a small crystal of composition Ce-Ti-Si-O which was identifiable using a diffraction tilt series as the silicate  $\text{Ce}_2\text{Ti}_2(\text{Si}_2\text{O}_7)\text{O}_4$  (JCPDS #19-302). The Ti in this compound may have originated in a binder present in the zeolite. Rare earth silicates such as that shown in Fig. 1 were present in all cold surrogate CWF samples. In addition, small quantities of  $\text{ZrO}_2$  and  $\text{ZrSiO}_4$  were identified using EDX and TED. As is the

case in Fig. 1, the silicates had a tendency to be within or in contact with the glass phase. In many cases, clusters of small silicate crystals were also observed. Larger single crystals of rare earth silicates with sizes of several microns were also occasionally encountered. Finally, a minor quantity of spherical NaCl crystals were found dispersed within the glass phase (see Fig. 4, below). In spite of the mottled appearance these crystals, they were found by diffraction to be single crystals with halite structure.

The volume fraction of rare earth silicate crystals is small and is estimated at significantly less than 1 vol% of the entire sample. This is in rough agreement with the small concentration of rare earth elements in the overall mixture. Assuming that all rare earths transform to silicates with a volume of approximately  $0.5 \text{ m}^3$  per mole of rare earth atoms, the volume fraction of rare earth silicate in the final sample would be of the order of 0.1 %. Due to the difficulty of accurately estimating a small volume fraction, it is nevertheless possible that some quantity of the rare earths were absorbed into the sodalite or glass phases at concentrations not detectable by EDX.

#### b) $^{239}\text{Pu}$ loaded CWF

The salt composition in the case of pellet HUP 24 was much simpler than for the surrogate CWF samples, and consisted purely of the LiCl - KCl eutectic salt, plus an additional quantity of  $\text{PuCl}_3$ . Nevertheless, strong parallels to the surrogate CWF were found in the microstructure, with  $\text{PuO}_2$  taking the place of the rare earth silicates. A BFI of the microstructure of HUP 24 is shown in Fig. 4. The image shows a polycrystalline sodalite region approximately  $2.5 \mu\text{m}$  in diameter, which is partially surrounded by glass regions. In addition to the predominant polycrystalline sodalite/glass microstructure, the only other phases present in the sample were  $\text{PuO}_2$  with the cubic fluorite structure, present as small particles in the glass phase, and spherical NaCl crystals. EDX spectra of the glass and sodalite phases were similar to those seen in the surrogate CWF (Figs. 2 and 3). The EDX scans indicate minimal occlusion of Pu in the sodalite. No examples of a sodalite phase with detectable Pu were found. The EDX spectrum from a  $\text{PuO}_2$  particle shown in Fig. 5 is dominated by characteristic lines of Pu, with possible impurity lines as well as Al, Si and Cl peaks arising from scattering from the adjacent glass phase.

The morphology and size of the sodalite region in Fig. 4 suggests that it formed from what was a single zeolite powder grain at the salt blending stage. The grains of  $\text{PuO}_2$  in the microstructure consistently tended to cluster in the glass phase near the glass/sodalite boundary, as is evident in the Fig. 4. This distribution of the  $\text{PuO}_2$  grains suggests that the Pu becomes concentrated within a surface layer on the zeolite grains in the salt blending process. The formation of  $\text{PuO}_2$  at the blending stage is also consistent with the appearance of  $\text{PuO}_2$  in x-ray diffraction patterns of the salt-blended zeolite. The  $\text{PuO}_2$  particles were frequently found in the glass slightly displaced from the glass/sodalite boundary. This suggests that interaction between the glass and sodalite phases during the HUP process leads to dissolution of a small amount of sodalite, leaving the  $\text{PuO}_2$  particles marking the position of the initial glass/zeolite boundary. This interpretation is also consistent with the change in the glass phase composition mentioned above.

The presence of a large number of fine crystals of  $\text{PuO}_2$  indicates that reaction of Pu-chloride in the molten salt to form oxide is preferred over incorporation of Pu into either the sodalite or glass phases. The likely mechanisms for such a reaction are either via oxygen exchange with residual water from the zeolite, or possibly via combination of Pu with oxygen native to the zeolite (attack of the zeolite). Residual water in the zeolite was determined prior to producing the sample to be 0.25 wt%, which is less than half that needed to react with all the Pu from the salt to form  $\text{PuO}_2$ . Nevertheless, zeolite 4A can absorb water from the argon glovebox atmosphere in the course of processing, so it is difficult to rule out the absorption of a small quantity of additional water. In addition, the reaction of  $\text{PuCl}_3$  with water to form  $\text{PuO}_2$  plus gaseous HCl is extremely

exothermic [4], so that if enough water were present, it would be the preferred reaction mechanism. In the absence of sufficient water, it is also possible that Pu may acquire oxygen native to the zeolite via anion exchange with Na of the zeolite to form NaCl, accompanied by the production of an amorphous phase from the remaining zeolite components. In the case of the actual planned CWF, to be produced in a hot cell at ANL-W, the typical zeolite water content will be  $\approx 1$  wt%, and will always be sufficient to transform all Pu-chloride to  $\text{PuO}_2$ .

Assuming that all Pu was transformed to  $\text{PuO}_2$  in this sample, the ratio between the volume of sodalite phase to that of  $\text{PuO}_2$  should be on the order of 0.6%. This is consistent with the amount of  $\text{PuO}_2$  observed in this sample, which clearly exceeded that of the rare earth silicate component in the cold surrogate CWF presented above. The overall concentration of Pu in both HUP 24 and HUP 36 below is approximately 3.4 wt%, significantly more than the Pu levels of 0.2 - 1 wt% anticipated in the actual CWF.

#### c) $^{238}\text{Pu}$ loaded CWF

An initial TEM study of the  $^{238}\text{Pu}$  sample CL036 was conducted, with additional examinations planned as part of a longer term study of the effects of  $\alpha$  and recoil damage in the CWF. Overall, the microstructure is similar to that found in the  $^{239}\text{Pu}$  sample, with a number of minor exceptions. Fig. 6a shows a low magnification BFI of the sample, in which both polycrystalline sodalite and glass regions are visible. A number of dark crystals are observed in the image. These are clearer in Fig. 6b, which is an image of the same area taken with the objective aperture removed so that the contrast is dominated by the strong absorption in Pu-rich crystals. All dark crystals investigated contained Pu, which is by far the most prevalent heavy element in the sample. As can be seen, and in contrast to HUP 24, there is a significant number of small Pu-rich crystals as intergranular particles in the sodalite region.

Diffraction patterns from the smaller dark crystals with sizes in the 10 nm - 50 nm range were uniformly indexable to the cubic fluorite structure. However, a number of the larger Pu-containing crystals were distinct both compositionally and structurally. An EDX spectrum is shown in Fig. 7, which clearly contrasts with Fig. 5 above in the presence of strong Si, Al and Cl peaks. A distinct composition of a number of the larger crystals in Fig. 6b is also suggested by their lighter appearance. Diffraction tilt series on this phase were consistently indexable to a body-centered tetragonal unit cell with  $a \approx 4.1$  Å and  $c/a \approx 1.36$ . The patterns were not indexable to any oxide, chloride, oxychloride, silicide or silicate phase of plutonium [5], or to a large number of rare earth silicates and oxides considered to date. Features consistent with this phase were also observed using SEM from this sample [2], but were not observed in HUP 24. Definitive identification of this unknown phase is planned at later stages of the irradiation study.

## CONCLUSIONS

Microstructure characterization of the CWF developed for disposition of salts generated during electrometallurgical treatment of EBR II SNF has indicated that the samples are dominated by polycrystalline sodalite and amorphous regions. Absorption of the major components of the salt within the sodalite and glass phases accomplishes the desired reduction in the quantity of free chlorides. The Pu-chloride in the salt transforms during salt blending to  $\text{PuO}_2$ , which is found in the final waste form as small grains in the glass phase predominantly adjacent to sodalite regions.

## ACKNOWLEDGMENTS

Argonne National Laboratory is operated for the US Department of Energy by the University of Chicago. This work was supported by the Department of Energy, Nuclear Energy Research and

Development Program, under contract no. W-31-109-ENG-38. The authors wish to thank M. Simpson and K. Bateman for producing the waste forms and providing processing information.

REFERENCES

- 1) J. P. Ackerman, T. R. Johnson, L. S. H. Chow, E. L. Carls, W. H. Hannum and J. J. Laidler, "Treatment of Wastes in the IFR Fuel Cycle", Prog. Nucl. Energy 31 (1997) 141-154.
- 2) T. L. Moschetti, T. P. O'Holleran, S. M. Frank, S. G. Johnson, D. W. Esh and K. M. Goff, "Plutonium & Surrogate Fission Products in Composite Ceramic Waste Form", This proceedings.
- 3) S. M. Frank, K. Bateman, T. DiSanto, S. G. Johnson, T. Moschetti, M. Noy and T. P. O'Holleran, "Characterization of Composite Ceramic High-Level Waste Forms", in *Phase Transformations and Systems Driven Far From Equilibrium*, MRS Symp. Proc. vol 481, E. Ma, P. Bellon, M. Atzmon, R. Trivedi. eds., MRS, Pittsburgh, 1998 pp. 351-356.
- 4) M Richmann, personal communication.
- 5) Roof, R. B. "X-Ray Diffraction Data for Plutonium Compounds, Vol. 3, Ternary Compounds". LAUR 11619, Los Alamos National Laboratory, 1989

Table 1. Sample processing. Conditions given for cold surrogates are typical of a larger number of samples.

sample	salt w%	zeolite w%	glass w%	blending T (°C)	blending time (h)	pressing time (h)	T <sub>max</sub> (°C)	P <sub>max</sub> (ksi)
coldHUP	7.5	67.5	25	500	20	1	750	10.2
cold HIP	7.5	67.5	25	500	20	1	850	14.5
HUP 24	10.2	64.8	25	500	48	2	750	5.1
HUP 36	10.2	64.8	25	500	34	4	750	5.1

Table 2. Cold surrogate salt

salt compound	wt%
LiCl	45.3
KCl	40.1
NaCl	6.1
KBr	0.015
RbCl	0.13
SrCl <sub>2</sub>	0.42
YCl <sub>3</sub>	0.26
KI	0.065
CsCl	1.0
BaCl <sub>2</sub>	0.45
LaCl <sub>3</sub>	0.48
CeCl <sub>3</sub>	3.4
PrCl <sub>3</sub>	0.46
NdCl <sub>3</sub>	1.5
SmCl <sub>3</sub>	0.26
EuCl <sub>3</sub>	0.017

Table 3. Pellet HUP 24 salt

salt compound	wt%
LiCl	33.2
KCl	29.5
<sup>239</sup> PuCl <sub>3</sub>	37.3

Table 4. Pellet HUP 36 salt

salt compound	wt%
LiCl	26.250
KCl	23.279
<sup>238</sup> PuCl <sub>3</sub>	35.474
NaCl	2.484
<sup>239</sup> PuCl <sub>3</sub>	8.046
NdCl <sub>3</sub>	1.139
CsCl	0.736
CeCl <sub>3</sub>	0.682
SrCl <sub>2</sub>	0.295
BaCl <sub>2</sub>	0.350
LaCl <sub>3</sub>	0.357
PrCl <sub>3</sub>	0.337
YCl <sub>3</sub>	0.205
RbCl	0.097
SmCl <sub>3</sub>	0.200
KBr	0.007
KI	0.045

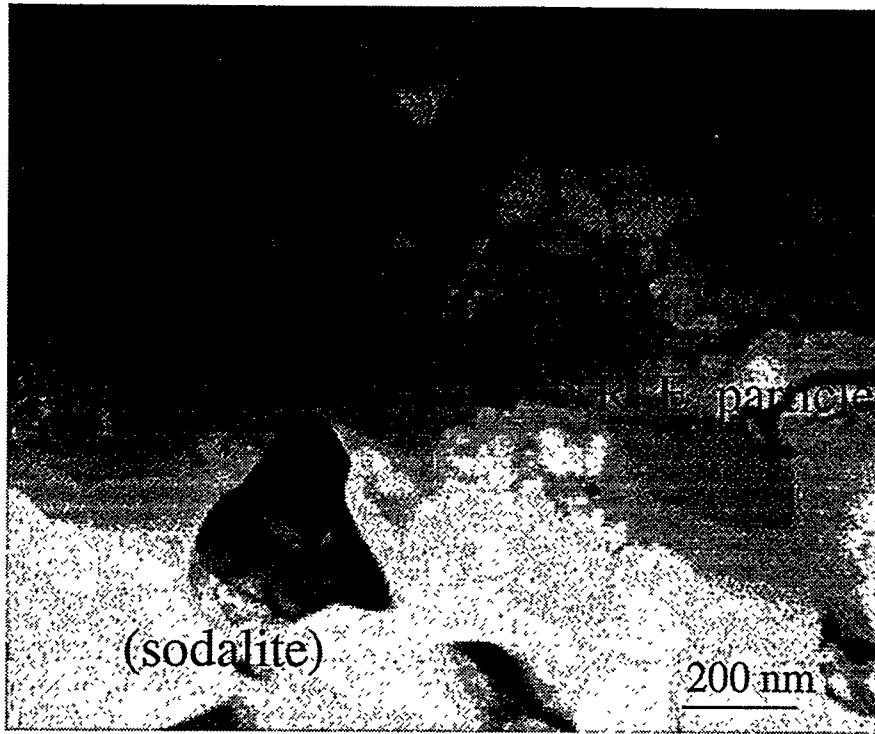


Fig. 1. Microstructure image from cold surrogate HIP can.

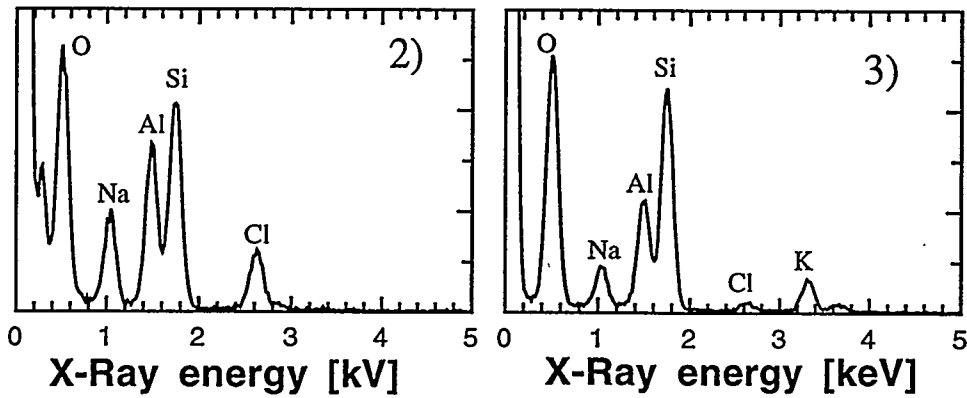


Fig. 2. Typical sodalite EDS spectrum from surrogate CWF.

Fig. 3. Typical glass EDS spectrum from surrogate CWF.

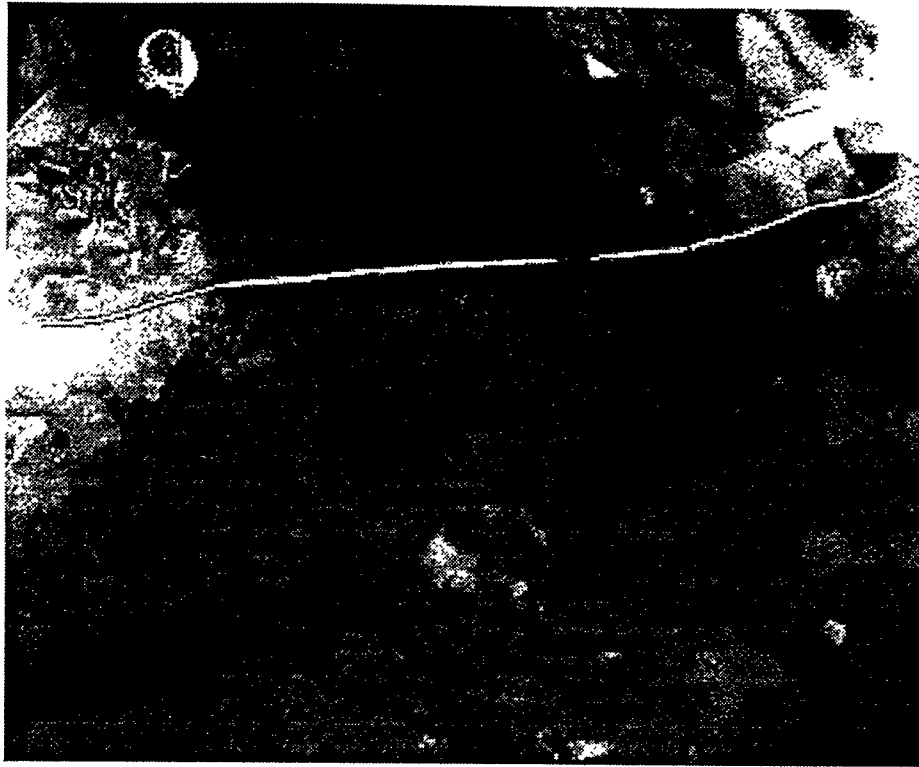


Fig. 4. BFI of sample CLO24 microstructure. Regions marked "g" are Amorphous, regions marked "s" are sodalite. Small dark crystals (predominantly near edges of sodalite regions) are  $\text{PuO}_2$ . A NaCl crystal is also visible in the glass phase (h).

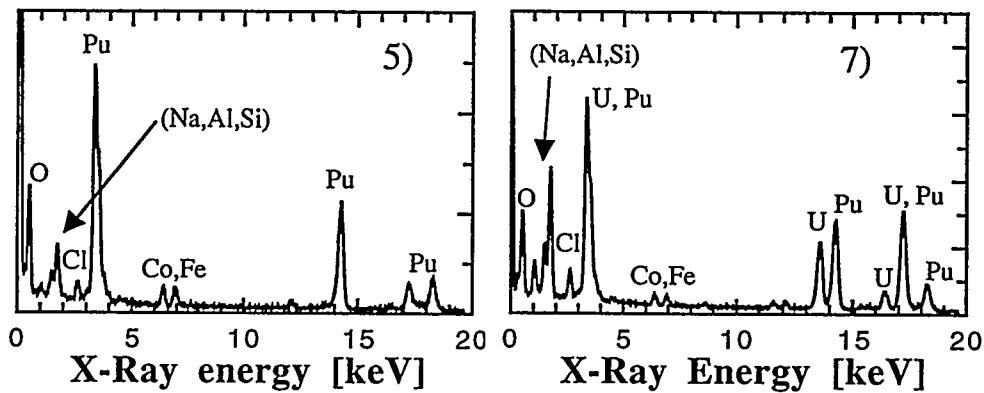


Fig. 5. EDX spectrum of  $\text{PuO}_2$  phase in HUP 24

Fig. 7. EDX spectrum from a particle of unidentified tetragonal phase. Uranium peaks are from decay of  $^{238}\text{Pu}$ .

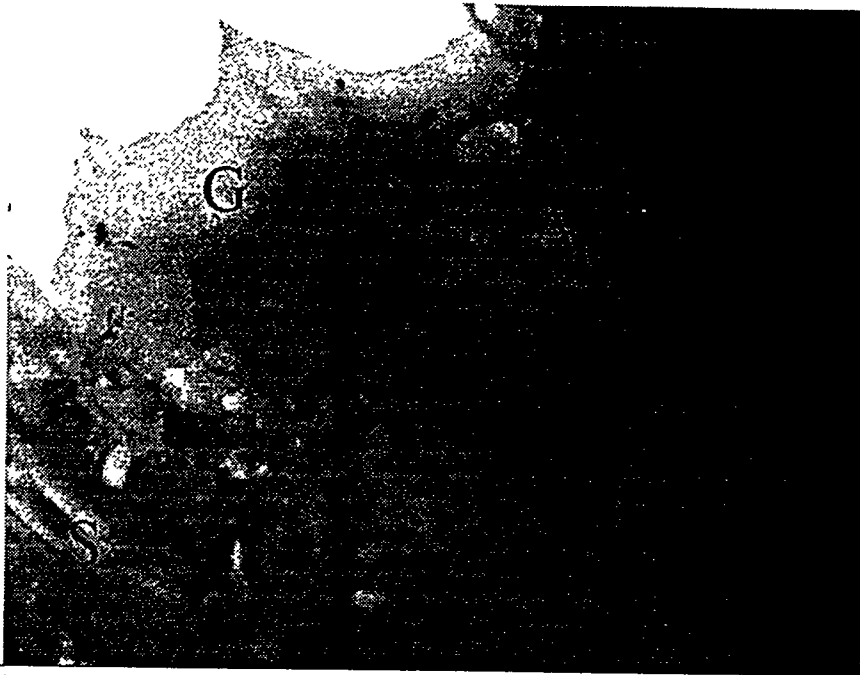


Fig. 6a. Typical microstructure image of sample HUP 36. G=glass, S=sodalite. The smaller dark crystals were generally found to be  $\text{PuO}_2$ . A is a large single crystal of sodalite, devoid of  $\text{PuO}_2$  particles.

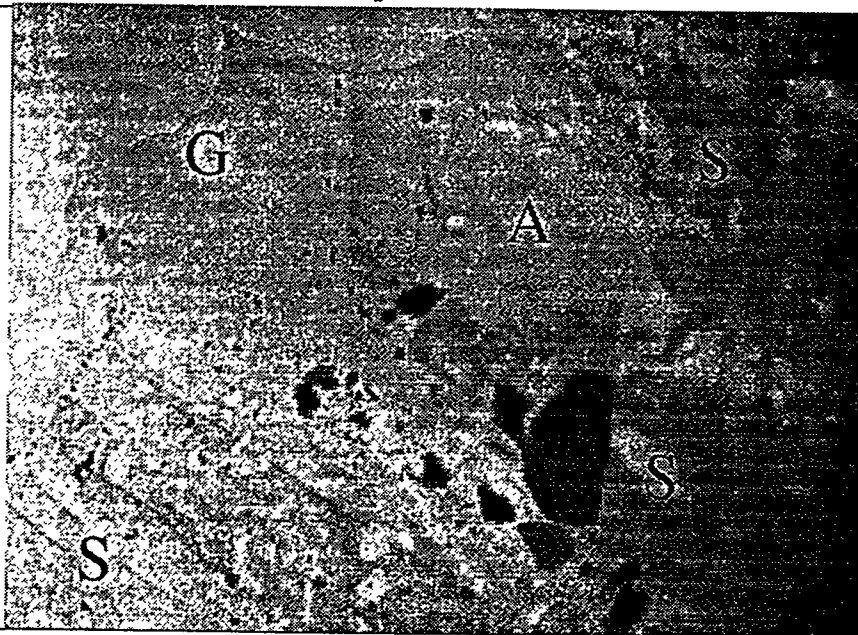


Fig. 6b. Same as Fig. 9a, but with contrast dominated by absorption properties. Large dark crystals are visible in contact with sodalite. These may be either  $\text{PuO}_2$  or unknown tetragonal phase (see text).